

Synthesis, Structure, and Electrical Properties of New Homo and Heteronuclear Schiff Base Copper(II) and Nickel(II) Complexes

T. Topal^{a,*}, N. Karapınar^b, D. Takanoglu Bulut^c, and E. Karapınar^a

^a Department of Chemistry, Pamukkale University, Denizli, 20020 Turkey

^b Department of Chemical Engineering, Pamukkale University, Denizli, 20020 Turkey

^c Department of Physics, Pamukkale University, Denizli, 20020 Turkey

*e-mail: ttopal@pau.edu.tr

Received September 4, 2020; revised March 24, 2021; accepted June 22, 2021

Abstract—In this study, the new Schiff base ligands *N,N'*-bis[(1*Z*,2*E*)-1-(4-methylphenyl)-2-(hydroxyimino)-1-phenylethylidene]-4-methylbenzene-1,2-diamine and *N,N'*-bis[(1*Z*,2*E*)-1-(4-chlorophenyl)-2-(hydroxyimino)ethylidene]-4-methylbenzene-1,2 diamine have been synthesized. Their metal complexes with copper and nickel have been formed and characterized by FT-IR, UV-Vis, NMR, LC/MS-MS spectra, molar conductivity, magnetic susceptibility, elemental analysis, ICP-OES, and thermogravimetric analysis. The complexes demonstrate semi-conducting features.

Keywords: transition metal complexes, Schiff-base ligands, electrical characterization

DOI: 10.1134/S1070363221060207

INTRODUCTION

Many Schiff bases were used as ligands in preparation of complexes with copper, nickel, cobalt, and iron [1, 2]. Synthetic organic semiconductors are widely used in electronic industry [3–5]. In this study, newly synthesized organic oxime-containing metal complexes were synthesized and their temperature-dependent electrical parameters studied.

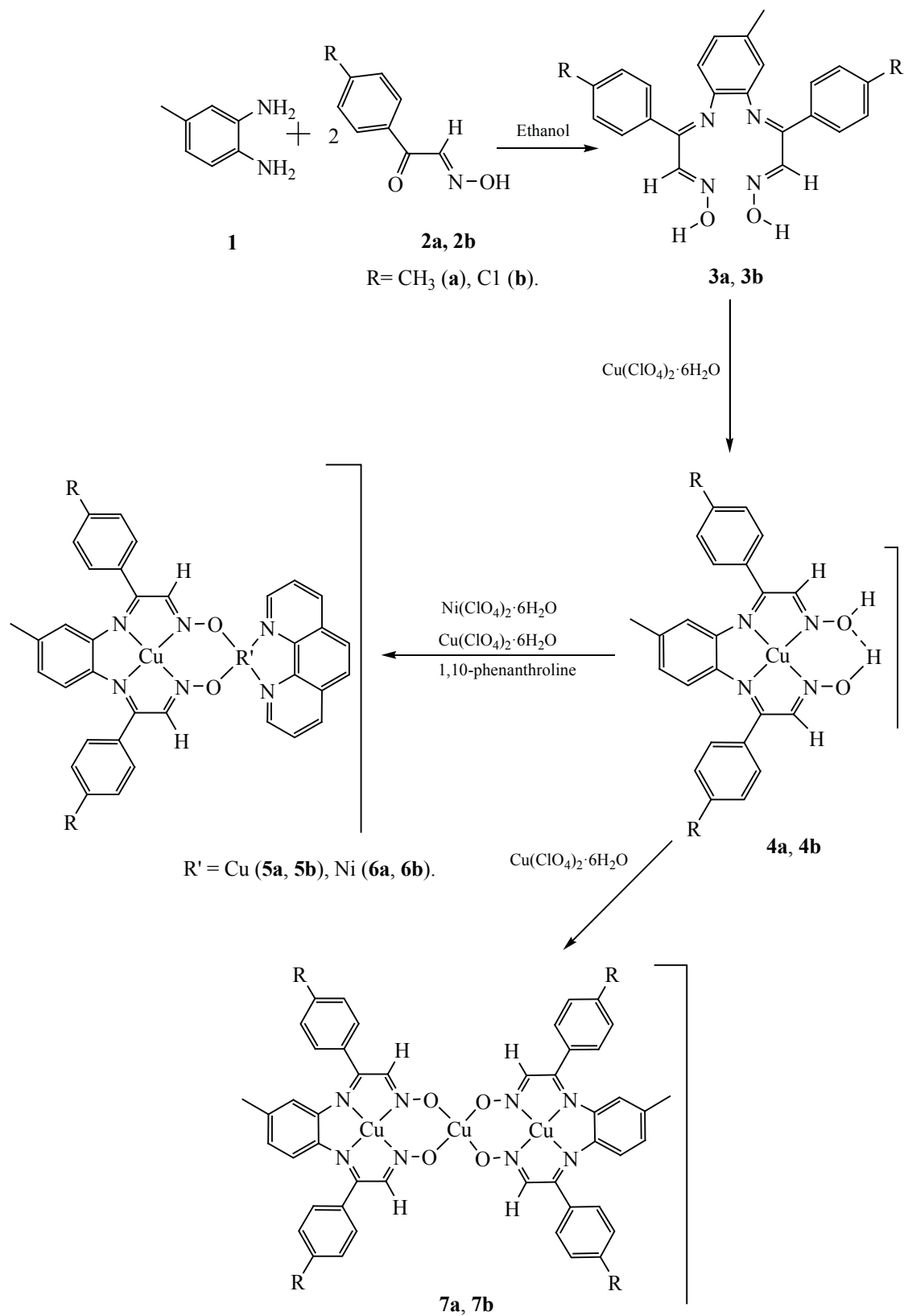
RESULTS AND DISCUSSION

Earlier, we have studied reactions of isonitrosomethyl-*p*-tolyl ketone with 1,2-diaminobenzene and its metal complexes [6]. Herein, we report reactions of isonitroso-*p*-chloroacetophenone **2a** and isonitroso-*p*-methylacetophenone **2b** with 3,4-diaminotoluene in ethanol that led to formation of oximes **3a**, **3b** [7, 8]. Structures of the synthesized ligands were supported by IR, UV-Vis, and NMR spectroscopy, LC/MS-MS, elemental analysis, thermal analyses. In mononuclear complexes **4a** and **4b** Cu(II) ion was coordinated to nitrogen and oxygen atoms of the imine and oxime groups of the ligands. The compounds **4a** and **4b** were reacted with Cu(II) and Ni(II) perchlorates to obtain

complexes **5a**, **5b**, **6a**, **6b**, **7a**, and **7b** (Scheme 1). In the homodinuclear **5a** and **5b** and heterodinuclear **6a** and **6b** complexes, second metal ions [Cu(II) or Ni(II)] coordinated with 1,10-phenanthroline nitrogen atoms. Homotrimeric copper complexes **7a** and **7b** were formed by the combination of three Cu(II) ions with diimine-dioximes [9, 10]. Mononuclear complexes had the square pyramidal geometry, but we could not suggest any coordination geometry for the other complexes. The resulting complexes were readily soluble in methanol, ethanol, acetone, and chloroform but poorly soluble in water and ether [11]. Electrical conductivity of the synthesized complexes was studied in the temperature range of 300–400 K [12].

¹H and ¹³C NMR spectra supported the structures of the ligands [13–17]. In IR spectra the bands of the (C=N)_{imine} and (C=N)_{oxime} groups recorded for **3a** and **3b** ligands in the ranges of 1608–1620 and 1576–1593 cm⁻¹ were shifted to the lower frequencies upon complexation indicating that oxime and imine nitrogen atoms were coordinated to the metal ions [28]. Due to the fact that the mononuclear complexes were coordinated via nitrogen atoms, the M–O band was not observed.

Scheme 1. Synthetic approaches to the complexes.



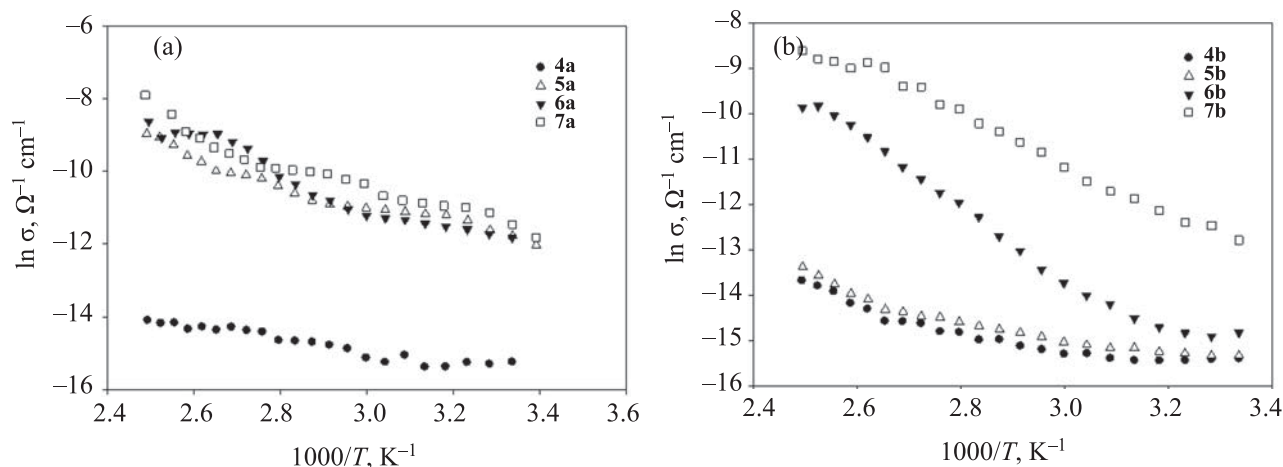


Fig. 1. Temperature dependence of electrical conductivity of **3a** (a) and **3b** (b) series.

In TGA experiments all complexes demonstrated the gradual weight loss upon heating. Generally, thermograms of the complexes were characterized by three or four decomposition steps within the temperature range 35–900°C. The first and second weight losses (75–175°C)–(175–240°C) were assigned to the lattice and coordinated water molecules. The third step in the range of 240–340°C indicated decomposition of the coordinated ligands. The fourth weight loss (400–900°C) indicated formation of the corresponding metal oxides [18–20].

Molar conductivity measurements were carried out at 25°C and used 2×10^{-5} mol methanol solutions, and the accumulated data for the complexes fall between 174 and $642 \Omega^{-1} \text{ cm}^2 \text{ mol}^{-1}$ which did not allow to establish a correlation between the copper-nickel ratios and molar conductivity [21].

The magnetic moments measured for mononuclear Cu(II) complexes **4a**, **4b** (1.84 and 1.90 B.M.) corresponded to one unpaired electron. The magnetic moments measured for homodinuclear complexes **5a** and **5b** (2.01 and 2.16 B.M.), heterodinuclear complexes **6a** and **6b** (2.91 B.M. and 2.94 B.M.) and trinuclear complexes **7a** and **7b** (1.71 and 1.81 B.M.) indicated their paramagnetic character. The data accumulated for trinuclear and dinuclear complexes were lower than magnetic moments equivalent to three and two electrons, which could be due to the strong intramolecular antiferromagnetic effect [22].

In UV-Vis spectra of **3a** and **3b** ligands the bands were recorded at 276 and 285 nm ($\epsilon = 32120$ and $30960 \text{ mol}^{-1} \text{ L cm}^{-1}$) and assigned to the aromatic rings

$n-\pi^*$ transitions. The bands at 314 and 333 nm ($\epsilon = 22340$ and $25520 \text{ mol}^{-1} \text{ L cm}^{-1}$) were attributed to the imine and oxime $\pi-\pi^*$ transitions [21]. The absorption bands between 337 and 983 nm were attributed to ligand-to-metal charge transfer bands of the d -orbitals of copper and nickel metal centers [23–25].

According to Figs. 1a, 1b, electrical conductivity of the samples increased exponentially upon heating, indicating their semiconducting behavior. The higher Cu rate resulted in increased conductivity of the samples. Electrical conductivity of the complexes of the **3b** series indicated their more stable behavior than that of the **3a** series being dependent upon Cu content and temperature.

Activation energies were calculated for the samples in the temperature range of 300–400 K. Resistivity and conductivity values determined for complexes of **3a** and **3b** series measured at room temperature are given in Table 1 [26].

Table 1. Some electrical parameters and activation energies of **3a** and **3b** series complexes measured at room temperature

Comp. no.	$\rho_{300}, \Omega \text{ cm}$	$\sigma_{300}, \Omega^{-1} \text{ cm}^{-1}$	$E_a, \text{ meV}$
4a	4.16×10^6	2.40×10^{-7}	203
5a	1.68×10^5	5.94×10^{-6}	325
6a	8.47×10^4	1.18×10^{-5}	234
7a	8.68×10^4	1.15×10^{-5}	202
4b	4.88×10^6	2.05×10^{-7}	160
5b	8.86×10^6	1.13×10^{-7}	163
6b	3.60×10^5	2.78×10^{-6}	517
7b	2.76×10^6	3.62×10^{-7}	698

EXPERIMENTAL

All reagents were purchased from Merck or Sigma-Aldrich and used without further purification. FT-IR spectra (400–4000 cm^{-1}) were recorded on a Perkin Elmer FTIR Spectrophotometer. UV-Vis spectra were recorded in chloroform on Shimadzu UV-1800 spectrophotometer within the wavelength range of 200–800 nm. NMR spectra were measured on a Varian 400 MHz NMR Spectrometer. Mass spectra [ESI] were measured on an Agilent Micromass Quattro LC-MS/MS spectrometer. Thermo Finnigan Flash EA 1112 Model analyzer was used to carry out elemental analysis. Quantitative analysis of copper and nickel ions was carried out on a PerkinElmer Inc. Optima 2000 DV ICP-OES device. Melting points were determined by a Stuart melting point SMP10 apparatus. Conductivity was measured in methanol on a WTW Conductivity 7110 meter. Magnetic moments were measured on a Sherwood Scientific MX1 Model. TGA was carried out on a Perkin-Elmer Diamond TGA System. Temperature-dependent electrical measurements were carried out on a Janis brand cryostat. Temperature control was provided by a LakeShore 331 temperature control unit.

Isonitroso-*p*-methylacetophenone **2a** and isonitroso-*p*-chloroacetophenone **2b** were prepared according to the published methods [8, 27, 28]. *N,N'*-Bis[(1*Z*,2*E*)-1-(4-methylphenyl)-2-(hydroxyimino)-1-phenylethylidene]-4-methylbenzene-1,2-diamine **3a** and *N,N'*-bis[(1*Z*,2*E*)-1-(4-chlorophenyl)-2-(hydroxyimino)ethylidene]-4-methylbenzene-1,2-diamine **3b** were obtained according to the procedure described in [29]. All complexes were obtained by the modified previously reported method [6].

***N,N'*-Bis[(1*Z*,2*E*)-1-(4-methylphenyl)-2-(hydroxyimino)-1-phenylethylidene]-4-methylbenzene-1,2-diamine (3a).** Yield 69%, mp 120–122°C. IR spectrum, ν , cm^{-1} : 3227 (OH), 1671 (C=N, imine), 1606 (C=N, oxime), 1057 (=N–O). ^1H NMR spectrum (CDCl_3), δ , ppm: 2.45 s (6H) (Ar-CH_3), 2.60 s (3H) ($\text{Ar}_{\text{amine}}\text{-CH}_3$), 7.35–8.08 m (11H, H_{arom}), 8.09 s (1H, H–C=N), 8.10 s (1H, H–C=N), 9.24 s (1H, OH), 9.26 s (1H, OH). ^{13}C NMR spectrum, δ_{C} , ppm: 21.40, 21.80, 21.84, 126.96, 127.27, 127.35, 127.93, 128.38, 128.55, 129.02, 129.83, 131.58, 132.47, 134.13, 139.80, 139.91, 140.18, 140.31, 140.68, 140.75, 141.46, 142.37, 143.16, 151.03, 151.73. Found, %: C 72.74; H 5.82; N 13.64. $\text{C}_{25}\text{H}_{24}\text{N}_4\text{O}_2$. Calculated, %: C 72.80; H 5.86; N 13.58. MS (MM): m/z : 412.48 [$M - 2$] $^+$. UV–Vis spectrum (CH_2Cl_2): 276 (32120), 314 (22340).

***N,N'*-Bis[(1*Z*,2*E*)-1-(4-chlorophenyl)-2-(hydroxyimino)ethylidene]-4-methylbenzene-1,2-diamine (3b).** Yield 67%, mp 150–152°C. IR spectrum, ν , cm^{-1} : 3247 (OH), 1669 (C=N, imine), 1592 (C=N, oxime), 1011 (=N–O). ^1H NMR spectrum (CDCl_3), δ , ppm: 2.59 s (3H) ($\text{Ar}_{\text{amine}}\text{-CH}_3$), 7.55–8.02 m (11H, H_{arom}), 8.04 s (1H, H–C=N), 8.05 s (1H, H–C=N), 9.19 s (1H, OH), 9.21 s (1H, OH). ^{13}C NMR spectrum, δ_{C} , ppm: 21.88, 124.66, 124.78, 127.97, 128.38, 128.61, 128.81, 128.89, 129.06, 132.11, 132.25, 132.77, 135.73, 140.13, 140.41, 140.62, 141.03, 141.68, 141.84, 142.23, 142.64, 149.74, 150.46. Found, %: C 60.75; H 3.83; N 12.44. $\text{C}_{23}\text{H}_{18}\text{Cl}_2\text{N}_4\text{O}_2$. Calculated, %: C 60.94; H 4.00; N 12.36. MS (MM): m/z : 453.32 [$M - 3$] $^+$. UV–Vis spectrum (CH_2Cl_2): 285 (30960), 333 (25520).

[Cu(L₁)(H₂O)](ClO₄)₂·2H₂O (4a). Yield 59%, mp 200–202°C. IR spectrum, ν , cm^{-1} : 3705 (OH or H₂O), 2323 (O···H–H), 1610 (C=N, imine), 1576 (C=N, oxime), 1434 (=N–O), 1107, 1052, 619 (ClO₄), 481 (M–N). Found, %: C 42.02; H 4.31; N 7.74; Cu 8.78. $\text{C}_{25}\text{H}_{30}\text{Cl}_2\text{CuN}_4\text{O}_{12}$. Calculated, %: C 42.11, H 4.24, N 7.86, Cu 8.91. μ_{eff} B.M.: 1.84. $\Lambda_{\text{M}}^{\text{b}}$: 174. UV–Vis spectrum (CH_2Cl_2): 352 (41140), 636 (5340).

[Cu(L₂)(H₂O)](ClO₄)₂·2H₂O (4b). Yield 59%, mp 209–212°C. IR spectrum, ν , cm^{-1} : 3370 (H₂O or OH), 2323 (O···H–H), 1620 (C=N, imine), 1593 (C=N, oxime), 1492 (=N–O), 1089, 1046, 619 (ClO₄), 481 (M–N). Found, %: C 35.76; H 3.06; N 7.35; Cu 8.35. $\text{C}_{23}\text{H}_{24}\text{Cl}_4\text{CuN}_4\text{O}_{13}$. Calculated, %: C 35.88; H 3.14; N 7.28; Cu 8.25. μ_{eff} B.M.: 1.90. $\Lambda_{\text{M}}^{\text{b}}$: 393. UV–Vis spectrum (CH_2Cl_2): 349 (34890), 599 (41360), 780 (29630), 983 (8280).

[Cu(L₁)(H₂O)Cu(phen)](ClO₄)₂·(H₂O) (5a). Yield 61%, mp 278–281°C. IR spectrum, ν , cm^{-1} : 3542 (H₂O or OH), 1610 (C=N, imine), 1585 (C=N, oxime), 1432 (=N–O), 1091, 1050, 619 (ClO₄), 576 (M–O), 481 (M–N). Found, %: C 58.68; H 4.75; N 11.20; Cu 16.76. $\text{C}_{34}\text{H}_{24}\text{Br}_2\text{Cl}_2\text{Cu}_2\text{N}_6\text{O}_{11}$. Calculated, %: C 58.80; H 4.80; N 11.12; Cu 16.82. μ_{eff} B.M.: 2.01. $\Lambda_{\text{M}}^{\text{b}}$: 334. UV–Vis spectrum (CH_2Cl_2): 356 (33530), 635 (1560), 735 (12680), 766 (29610).

[Cu(L₂)(H₂O)Cu(phen)](ClO₄)₂ (5b). Yield 67%, mp 226–229°C. IR spectrum, ν , cm^{-1} : 3512 (H₂O or OH), 1620 (C=N, imine), 1591 (C=N, oxime), 1491 (=N–O), 1089, 1044, 620 (ClO₄), 572 (M–O), 484 (M–N). Found, %: C 43.11; H 2.79; N 8.49; Cu 12.89. $\text{C}_{35}\text{H}_{28}\text{Cl}_4\text{Cu}_2\text{N}_6\text{O}_{11}$. Calculated, %: C 43.00; H 2.89; N 8.60; Cu 13.00. μ_{eff} B.M.: 2.16. $\Lambda_{\text{M}}^{\text{b}}$: 438. UV–Vis

spectrum (CH₂Cl₂): 344 (31530), 599 (7620), 642 (7860), 833 (16980).

[Cu(L₁)(H₂O)Ni(phen)](ClO₄)₂·(H₂O) (6a). Yield 65%, mp >300°C. IR spectrum, ν , cm⁻¹: 3547 (H₂O or OH), 1608 (C=N, imine), 1582 (C=N, oxime), 1494 (=N–O), 1064, 620 (ClO₄), 573 (M–O), 497 (M–N). Found, %: C 46.71; H 3.76; N 8.75; Cu 6.59; Ni 6.12. C₃₇H₃₆Cl₂CuNiN₆O₁₂. Calculated, %: C 46.79; H 3.82; N 8.85; Cu 6.69; Ni 6.18. μ_{eff} B.M.: 2.91. $\Lambda_{\text{M}}^{\text{b}}$: 357. UV–Vis (CH₂Cl₂): 346 (23400), 635 (19450), 735 (9680), 766 (12590).

[Cu(L₂)(H₂O)Ni(phen)](ClO₄)₂ (6b). Yield 65%. mp 240–243°C. IR spectrum, ν , cm⁻¹: 3505 (H₂O or OH), 1620 (C=N, imine), 1592 (C=N, oxime), 1492 (=N–O), 1089, 1044, 620 (ClO₄), 571 (M–O), 493 (M–N). Found, %: C 43.37; H 3.02; N 8.50; Cu 6.42; Ni 5.94. C₃₅H₂₈Cl₄CuNiN₆O₁₁. Calculated, %: C 43.22; H 2.90; N 8.64; Cu 6.53; Ni 6.03. μ_{eff} B.M.: 2.94. $\Lambda_{\text{M}}^{\text{b}}$: 524. UV–Vis spectrum (CH₂Cl₂): 338 (17590), 596 (11840), 958 (2560).

[Cu₃(L₁)₂(H₂O)₂](ClO₄)₂·(H₂O)₂ (7a). Yield 60%, mp 236–238°C. IR spectrum, ν , cm⁻¹: 3563 (H₂O or OH), 1618 (C=N, imine), 1536 (C=N, oxime), 1465 (=N–O), 1096, 1047, 620 (ClO₄), 576 (M–O), 484 (M–N). Found, %: C 46.75; H 4.16; N 8.67; Cu 14.78. C₅₀H₅₂Cl₂Cu₃N₈O₁₆. Calculated, %: C 46.82; H 4.09; N 8.74; Cu 14.86. μ_{eff} B.M.: 1.71. $\Lambda_{\text{M}}^{\text{b}}$: 507. UV–Vis spectrum (CH₂Cl₂): 347 (15890), 594 (7260), 883 (22670), 980 (1450).

[Cu₃(L₂)₂(H₂O)₂](ClO₄)₂·(H₂O) (7b). Yield 57%. mp 238–240°C. IR spectrum, ν , cm⁻¹: 3582, 3550, 3511 (H₂O or OH), 1620 (C=N, imine), 1593 (C=N, oxime), 1491 (=N–O), 1089, 1047, 621 (ClO₄), 575 (M–O), 482 (M–N). Found, %: C 41.11; H 2.92; N 8.26; Cu 14.08. C₄₆H₃₈Cl₆Cu₃N₈O₁₅. Calculated, %: C 41.04; H 2.85; N 8.32; Cu 14.16. μ_{eff} B.M.: 1.81. $\Lambda_{\text{M}}^{\text{b}}$: 642. UV–Vis spectrum (CH₂Cl₂): 337 (7500), 596 (1200), 650 (17650), 964 (960).

CONCLUSIONS

Structures of the synthesized compounds are confirmed by spectroscopic and stoichiometric studies. The mononuclear complexes are formed via nitrogen atoms of the imine and oxime groups of the ligands. The initially produced complexes have been reacted with Cu(II) and Ni(II) perchlorates to give the corresponding homodinuclear, heterodinuclear and homotrimeric complexes. Electrical conductivity of the synthesized

complexes indicates that all complexes have semiconductor properties.

FUNDING

This study has been supported by Pamukkale University (grant nos. 2015HZL014)

CONFLICT OF INTEREST

No conflict of interest was declared by the authors.

REFERENCES

- Karapinar, E., *J. Incl. Phenom.*, 2005, vol. 53, p. 171. <https://doi.org/10.1007/s10847-005-2548-z>
- Allan, J.R., Gardner, A.R., McCloy, B., and Smith, W.E., *Thermochim. Acta*, 1992, vol. 208, p. 125., [https://doi.org/10.1016/0040-6031\(92\)80158-S](https://doi.org/10.1016/0040-6031(92)80158-S)
- Aydogdu, Y., Yakuphanoglu, F., Aydogdu, A., Tas, E., and Cukurovali, A., *Solid State Sci.*, 2002, vol. 4, p. 879. [https://doi.org/10.1016/S1293-2558\(02\)01298-0](https://doi.org/10.1016/S1293-2558(02)01298-0)
- Aydogdu, Y., Yakuphanoglu, F., Aydogdu, A., Tas, E., and Cukurovali, A., *Mater. Lett.*, 2003, vol. 57, p. 3755. [https://doi.org/10.1016/S0167-577X\(03\)00174-5](https://doi.org/10.1016/S0167-577X(03)00174-5)
- Aydogdu, Y., Yakuphanoglu, F., Aydogdu, A., Temel, H., Sekerci, M., and Hosgoren, H., *Solid State Sci.*, 2001, vol. 3, p. 377. [https://doi.org/10.1016/S1293-2558\(00\)01143-2](https://doi.org/10.1016/S1293-2558(00)01143-2)
- Topal, T. and Karapinar, E., *J. Turkish Chem. Soc. Sect. A: Chem.*, 2018, vol. 5, p. 785. <https://doi.org/10.18596/jotcsa.324878>
- Demir, I. and Pekacar, A., *Synth. React. Inorg. Met. Nano-Metal. Chem.* 2005, vol. 35, p. 825. <https://doi.org/10.1080/15533170500358234>
- Sevindir, H.C. and Mirzaoglu, R., *Synth. React. Inorg. Met. Chem.*, 1992, vol. 22, p. 851. <https://doi.org/10.1080/15533179208020249>
- Dede, B., Ozmen, I., and Karipcin, F., *Polyhedron*, 2009, vol. 28, p. 3967. <https://doi.org/10.1016/j.poly.2009.09.020>
- Topal, T., *PhD Thesis (Chemistry)*, Pamukkale University, Denizli, 2016.
- Chapurkin, V.V., Rakhimov, A.I., Vaniev, M.A., Chapurkin, S.V., and Borisov, S.V., 2020, *Russ. J. Gen. Chem.*, vol. 90, p. 1188. <https://doi.org/10.1134/S1070363220070026>
- Karapinar, E., Karabulut, O., and Karapinar, N., *Hindawi Publ. Corp. J. Chem.*, 2013, vol. 2013, <https://doi.org/10.1155/2013/256983>
- Maksimov, A.F., Zhukova, A.A., Ernandes, A.M.P., Kuttyreva, M.P., Gataulina, A.R., and Kuttyrev, G.A.,

- Russ. J. Gen. Chem.*, 2020, vol. 90, p. 1285.
<https://doi.org/10.1134/S1070363220070142>
14. Dede, B., Karipcin, F., and Cengiz, M., 2009, *J. Hazard. Mater.*, vol. 163, p. 1148.
<https://doi.org/10.1016/j.jhazmat.2008.07.070>
15. Dede, B., Karipcin, F., and Cengiz, M., *J. Chem. Sci.*, 2009, vol. 121, p. 163.
<https://doi.org/10.1007/s12039-009-0018-7>
16. Karaböcek, N., Armutcu, A., and Karaböcek, S., *Transit. Met. Chem.*, 2006, vol. 31, p. 938.
<https://doi.org/10.1007/s11243-006-0089-y>
17. Prushan, M., Addison, A., Butcher, R., and Thompson, L., *Inorganica Chim. Acta*, 2005, vol. 358,
<https://doi.org/10.1016/j.ica.2005.04.038>.
18. Rahmatabadi, F.D., Khojasteh, R.R., Fard, H.K., and Tadayon, F., *Russ. J. Gen. Chem.*, 2020, vol. 90, p. 1317.
<https://doi.org/10.1134/S1070363220070191>
19. Onac, C., *Electroanalysis*, 2020, vol. 32, p. 1315.
<https://doi.org/10.1002/elan.201900755>
20. Yang, L., Zeng, L., Gu, W., Tian, J., Liao, Sh., Zhang, M., Wei, Z., Xin, L., and Liu, X., *Inorg. Chem. Commun.*, 2013, vol. 29, p. 76.
<https://doi.org/10.1016/j.inoche.2012.12.015>
21. Demir, I., Diler, S.B., and Uçan, S.Y., *Russ. J. Gen. Chem.*, 2020, vol. 90, p. 1051.
<https://doi.org/10.1134/S1070363220060183>
22. Kulkarni, N.D. and Bhattacharya, P.K., *Transit. Met. Chem.*, 1989, vol. 14, p. 303.
<https://doi.org/10.1007/BF01098235>
23. Sennappan, M., Murali Krishna, P., Hosamani, A.A., and Hari Krishna, R., *J. Mol. Struct.*, 2018,
<https://doi.org/10.1016/j.molstruc.2018.03.054>
24. Chai, L.Q., Zhang, J.Y., Chen, L.C., Li, Y.X., and Tang, L.J., *Res. Chem. Intermed.*, 2016, vol. 42, p. 3473.
<https://doi.org/10.1007/s11164-015-2226-8>
25. Sağlam, E.G., Dal, H., Mougang-Soumé, B., and Hökelek, T., *J. Mol. Struct.*, 2020, vol. 1202, p. 127222.
<https://doi.org/10.1016/j.molstruc.2019.127222>
26. Takanoglu, D., Yilmaz, K., Ozcan, Y., and Karabulut, O., *Chalcogenide Lett.*, 2015, vol. 12, p. 35.
27. Karapinar, E. and Özcan, E., *J. Incl. Phenom.*, 2003, vol. 47, p. 59
<https://doi.org/10.1023/B:JIPH.0000003926.35770.2c>
28. Pekacar, A. and Ozcan, E., *J. Macromol. Sci. - Pure Appl. Chem.*, 1994, p. 651.
29. Topal, T., Kart, H.H., Taşlı, P.T., and Karapinar, E., *Opt. Spectrosc.*, 2015, vol. 118, p. 897.
<https://doi.org/10.7868/S0030403415060227>